Atmos. Chem. Phys. Discuss., 12, 29607–29655, 2012
www.atmos-chem-phys-discuss.net/12/29607/2012/
doi:10.5194/acpd-12-29607-2012

Atmospheric Chemistry and Physics Discussions

Assessing the mineral dust indirect effects and radiation impacts on a simulated idealized nocturnal squall line

R. B. Seigel, S. C. van den Heever, and S. M. Saleeby

Department of Atmospheric Science, Colorado State University, 1371 Campus Delivery, Fort Collins, CO, 80523, USA

Received: 11 October 2012 – Accepted: 29 October 2012 – Published: 16 November 2012

Correspondence to: R. B. Seigel (rseigel@atmos.colostate.edu)

Published by Copernicus Publications on behalf of the European Geosciences Union.

Abstract

Mineral dust is arguably the most abundant aerosol species in the world and it plays a large role in aerosol indirect effects (AIEs). This study assesses and isolates the individual responses in a squall line that arise (1) from radiation, (2) from dust altering the microphysics, as well as (3) from the synergistic effects between (1) and (2). To accomplish these tasks, we use the Regional Atmospheric Modeling System (RAMS) set up as a cloud-resolving model (CRM). The CRM contains aerosol and microphysical schemes that allow mineral dust particles to nucleate as cloud drops and ice crystals, replenish upon evaporation and sublimation, be tracked throughout hydrometeor transition, and scavenge by precipitation and dry sedimentation.

Factor separation is used on four simulations of the squall line in order to isolate the individual roles of radiation (RADIATION), microphysically active dust (DUST MICRO), and the nonlinear interactions of those factors (SYNERGY). Results indicate that RADIATION acts to increase precipitation, intensify the cold pool, and enhance the mesoscale organization of the squall line due to changes in microphysics beginning from cloud top cooling. Conversely, DUST MICRO decreases precipitation, weakens the cold pool, and weakens the mesoscale organization of the squall line due to an enhancement of the warm rain process. SYNERGY shows little impact on the squall line, except near the freezing level, where an increase in mesoscale organization takes place. The combined effect of the mineral dust AIE due to both DUST MICRO and SYNERGY is to weaken the squall line.

1 Introduction

Aerosol can effectively serve as cloud condensation nuclei (CCN), giant cloud condensation nuclei (GCCN), and ice nuclei (IN) such that changes in the concentrations of these nuclei impact the microstructure and radiation budget of clouds and precipitating convection (Twomey, 1974; Albrecht, 1989). This is often referred to as the aerosol indirect effect (AIE) and is one of the largest uncertainties in cloud radiative forcing of the climate system (Forster et al., 2007; IPCC, 2007). Because of this, considerable research efforts have been made to better understand aerosol indirect effects on clouds and precipitation using both observations (e.g. Borys et al., 1998; Ferek et al., 2000; Kaufman and Nakajima, 1993; Heymsfield and McFarquhar, 2001; Rosenfeld, 1999, 2000; Andrae et al., 2005; Roselfeld et al., 2008) and models (e.g. Khain et al., 2005; Seifert and Beheng, 2006; van den Heever et al., 2006, 2011; Lee et al., 2008; Storer et al., 2010; Igel et al., 2012; Morrison, 2012; Storer and van den Heever, 2012). However, results from these studies have indicated that aerosol indirect effects are highly variable, demonstrating the sensitive nature of this problem (Rosenfeld and Feingold 2003; Tao et al., 2012).

The original AIE theories (Twomey, 1974; Albrecht, 1989) were derived from studies of clouds that were comprised only of liquid water (i.e. warm clouds) – shallow cumulus and stratocumulus. These AIEs have been shown to include a reduction in precipitation for warm cloud systems when aerosols act only as CCN (Borys et al., 1998; Ferek et al., 2000; Kaufman and Nakajima, 1993; Rosenfeld, 2000; Heymsfield and McFarquhar, 2001). However, when aerosols are large enough to act as GCCN, the precipitation effects due to increased aerosol have been shown to reverse for warm clouds in polluted environments. For example, Feingold et al. (1999), Cheng et al. (2009), and Solomos et al. (2011) all found that when high concentrations of both CCN and GCCN were present, precipitation increased. Once clouds reach temperatures that allow for ice processes to become important, the AIE becomes increasingly complex as more microphysical processes are involved, and the impacts of aerosols acting as IN need to be considered. Because it is difficult to quantify the AIE of mixed-phase cloud systems observationally (Rosenfeld and Feingold, 2003; Matsui et al., 2004; Berg et al., 2008), numerous modeling studies have been performed to enhance our understanding of such effects (Khain et al., 2005; van den Heever et al., 2006, 2011; van den Heever and Cotton, 2007; Lee et al., 2008; Storer et al., 2010; Solomos et al., 2011; Igel et al., 2012; Morrison, 2012; Storer and van den Heever, 2012). However, results from these

ACPD
12, 29607–29655, 2012

studies have varied both in terms of convective invigoration and precipitation, which could be due to a number of factors (Morrison, 2012; Tao et al., 2012).

Despite the range in results that have been found for mixed-phase convective systems, a common factor amongst many of the modeling studies is that aerosols are typically represented as only one type of nucleating aerosol (Khain et al., 2005; van den Heever et al., 2011; Lee et al., 2008; Storer et al., 2010; Igel et al., 2012; Morrison, 2012; Storer and van den Heever, 2012). However, arguably the most abundant aerosol in our atmosphere, mineral dust (IPCC, 2001), has been found to act as CCN, GCCN, and IN (Twohy et al., 2009; DeMott et al., 2010), thereby potentially complicating the response. For example, van den Heever (2006) and van den Heever and Cotton (2007) both found that for continental deep convection, AIEs are highly variable and can change sign depending on the aerosol type involved.

While mineral dust is shown to have the highest concentrations close to its sources (desert regions) (Tegen and Fung, 1994), it has been observed to traverse the globe over vast distances (e.g. the Saharan Air Layer (SAL)) thereby impacting a variety of convective systems (Prospero, 1996, 1999; Perry et al., 1997; Sassen et al., 2003; van den Heever et al., 2006; Carrio et al., 2007; Bangert et al., 2012). One such system, which has been found to be the leading heavy-rain producer in the tropics and subtropics (Nesbitt et al., 2006), is the mesoscale convective system (MCS). While a number of studies have investigated AIEs on MCSs (Lynn et al., 2005a,b; Wang, 2005; Lee et al., 2008a,b, 2009a; Li et al., 2009), little investigation regarding the specific impacts of mineral dust on MCSs has been performed. This is surprising considering the high frequency of MCS occurrence near the primary dust source regions of the world (Nesbitt et al., 2006).

The primary goal of this study is to assess the aerosol indirect effects of mineral dust on squall lines. As with previous studies of the microphysical impacts on squall lines (Morrison et al., 2009; Bryan and Morrison, 2012; Morrison et al., 2012; Seigel and van den Heever, 2012b; van Weverberg et al., 2012) this will be achieved through idealized numerical modeling. In order to better our understanding of the mineral dust

ACPD
12, 29607–29655, 2012

AIE, recent model developments have been made to the microphysics and aerosol schemes in the model used in this study, the Regional Atmospheric Modeling System (RAMS). These now allow mineral dust particles to nucleate as both cloud drops and ice crystals (including immersion freezing), replenish upon evaporation and sublimation, be tracked throughout hydrometeor transition, and be scavenged by precipitation and dry sedimentation. This offers an excellent framework to explore in detail, the microphysical and radiative processes responsible for the AIEs of a mixed-phase cloud system, such as the squall line.

The role of radiation in squall line development and characteristics has been studied fairly extensively, the results of which indicate that radiation generally acts to strengthen squall lines due to increased instability from longwave cooling (Chen and Cotton, 1988; Dudhia, 1989; Tao et al., 1991, 1993; Chin, 1994; Dharssi et al., 1997). However, the role that radiation plays in squall lines due to *changes* in microphysical processes arising from the presence of aerosols is not well understood. Therefore, in order to isolate this role, as well as mineral dust AIEs on squall lines, a suite of idealized cloud resolving model simulations is performed. The analysis of these simulations utilize the technique of factor separation (Stein and Alpert, 1993; Alpert et al., 1995, 2011; Homar et al., 2003; van den Heever et al., 2006) to isolate the individual responses in the squall line that (1) arise from radiation, (2) from dust altering the microphysics, as well as (3) from the synergistic effects between (1) and (2). The following section will describe in detail the new microphysical model developments for representing mineral dust, along with an introduction to factor separation and its use in this study. Section 3 will present the results of the simulations and Sect. 4 will provide a discussion and summary of the work herein.

2 Methods

Four numerical simulations of an idealized squall line have been performed to assess the AIE of mineral dust. In order to obtain a realistic representation of mineral dust

ACPD
12, 29607–29655, 2012

within the cloud-resolving model (CRM) used for this study, modifications have been made to its microphysical scheme, the details of which are briefly described in this section following a short model description. Subsequently, the experimental design is presented.

2.1 Model description

Given that the AIE stems from aerosols modulating microphysical processes within clouds, it is important to use a model that best simulates the microphysical processes observed in reality. This has been demonstrated to be most accurate when using bin-resolved microphysics (Khain et al., 2000; Morrison and Grabowski, 2007), however the use of such schemes on scales that are required to simulate a three dimensional squall line (i.e. ~ 500 km) are too computationally expensive with our current computing technology. As such, a model that is appropriate to simulate both the microphysics and the dynamics of a squall line is the non-hydrostatic Regional Atmospheric Modeling System (RAMS; Pielke et al., 1992; Cotton et al., 2003; Saleeby and Cotton, 2004). RAMS has a sophisticated bin-emulating two-moment bulk microphysical parameterization scheme that prognoses mass mixing ratio and number concentration for eight hydrometeor species (cloud droplets, drizzle, rain, pristine ice, snow, aggregates, graupel, and hail) (Walko et al., 1995; Meyers et al., 1997; Cotton et al., 2003; Saleeby and Cotton, 2004). The representation of numerous hydrometeor species that all conform to a generalized gamma distribution (Flatau et al., 1989; Verlinde et al., 1990) helps to resemble the continuous spectrum of hydrometeors within the atmosphere.

In order to gain bin representation of various processes while maintaining computational efficiency, RAMS utilizes look-up tables that have been previously generated offline. These include hydrometeor sedimentation (Feingold et al., 1998), liquid-to-liquid, liquid-to-ice, and ice-to-liquid collisions (Feingold et al., 1988), and cloud droplet nucleation from aerosol within a detailed bin-resolving parcel model (Feingold and Heymsield, 1992; Saleeby and Cotton, 2004; Saleeby et al., 2012). Other schemes used in these simulations are radiative lateral boundary conditions (Klemp and Wilhelmson,

ACPD
12, 29607–29655, 2012

1978), a Rayleigh damping layer within the top six levels of the model domain with modifications by Lilly (1962) and Hill (1974), the Smagorinsky (1963) turbulence closure scheme, and Harrington (1997) two-strean radiation.

2.2 Mineral dust scheme

In RAMS, four aerosol species (ammonium sulfate, sodium chloride, mineral dust, and "regeneration") are represented. Mineral dust is unique in that the particles are predominantly insoluble and they often have large diameters, which helps to allow them to behave as CCN, GCCN, and IN (Twohy et al., 2009; DeMott et al., 2010). As such, care has been taken in the representation of mineral dust within RAMS to ensure that it behaves similarly to what is seen in reality. As described in detail by Saleeby and van den Heever (2012), the mineral dust scheme includes parameterizations for surface dust emission from wind and saltation, dry deposition, and wet scavenging by precipitation and nucleation.

Mineral dust is represented as two separate distributions; one small and one large mode, the details of which are described in the next subsection. For nucleation scavenging, the largest particles from the distribution are nucleated first and until supersaturation has been sufficiently reduced to halt nucleation (as is done with the other species). If a dust particle acts as a CCN that is less than or equal to 1 µm, then a cloud droplet is formed that contains a dust particle. Similarly, if a dust particle is larger than 1 µm the nucleated drop starts off as drizzle drop due to its large size; it also contains a dust particle. Because mineral dust is largely insoluble, the majority of the aerosol mass remains within the droplet in solid form and is then tracked through the various transitions between hydrometeor species. The insoluble mass within a drop is allowed to aid ice nucleation above the freezing level due to immersion freezing, which has shown to be an important ice nucleation mechanism (de Boer et al., 2010). Additionally, dry dust particles that have diameters greater than 0.5 µm are allowed to serve as IN, so long as the limit of activated IN at the respective temperature has not been

ACPD
12, 29607–29655, 2012

reached (DeMott et al., 2010). All heterogeneous nucleation of ice occurs following the parameterization of DeMott et al. (2010).

If a liquid drop or an ice crystal containing dust evaporates or sublimates, the dust mass is then added to the regenerated aerosol species. Due to the complicated nature of this aerosol regenerative process, assumptions have been made regarding the aerosol characteristics, as multiple aerosol species could be present in any drop. Saleeby and van den Heever (2012) provides a thorough description of the microphysical and aerosol schemes.

2.3 Experimental design

In this study, four idealized simulations are performed of a nocturnal squall line to investigate its response to the addition of mineral dust. All simulations are performed in three dimensions with a constant horizontal grid spacing of 500 m and a stretched vertical grid from 50 m to 500 m. The model domain covers a volume of 500 × 150 × 26 km in the zonal, meridional, and vertical directions, respectively. The time step used is 3 s and time integration is performed for 7 h nocturnally, as this is the peak occurence time of MCSs (Laing and Fritsch, 1997; Anderson and Arritt, 1998; Jirak et al., 2003).

Squall line initiation is performed from a similar framework as other previous idealized studies (Trier et al., 1997; Fierro et al., 2008; Morrison et al., 2009; Seigel and van den Heever, 2012b). The model domain is initialized with horizontally homogenous temperature and moisture profiles following Weisman and Klemp (1982), but with a boundary layer temperature profile that has been adjusted to mimic a well-mixed boundary layer, which better represents reality (Fig. 1). The shear profile used for initialization has a linear increase from 0 to 12.5 $\mathrm{m\,s^{-1}}$ in the lower 2.5 km (Fig. 1) and is within the range used by previous studies (Weisman, 1992, 1993; Weisman and Rotunno, 2004; Frame and Markowski, 2006; Bryan et al., 2007). The squall lines are initiated using a 4 km deep, −6 K line thermal resting on the surface, representing a cold pool, and contains random embedded $-0.1 \le \theta \le 0.1$ potential temperature (θ) perturbations to initiate three-dimensional motions.

Discussion Paper | Discussion Paper | Discussion Paper | Discussion Paper |

ACPD
12, 29607–29655, 2012

Aerosol data near one of the largest dust source regions in the world, the Sahara, is used to represent the nucleating species of sulfates and mineral dust within RAMS. These data have been collected from the NASA African Monsoon Multidisciplinary Analyses (NAMMA) experiment in 2006 (C. Twohy, personal communication, 2012), and are a good sampling of the SAL (DeMott et al., 2003). Figure 2 shows the vertical profiles and distributions (number and mass) of the aerosol concentrations for sulfate, small dust, and large dust particles. The treatment of dust for each simulation is described later in this subsection.

In order to more fully understand how mineral dust impacts the simulated squall line, factor separation (Stein and Alpert, 1993) is used to isolate the contributions from: (1) the inclusion of radiative transfer, while excluding mineral dust (herein referred to as RADIATION), (2) dust altering microphysical processes but not the subsequent radiative responses (herein referred to as DUST MICRO), and (3) the nonlinear interactions *between* dust altering microphysical processes and radiative transfer (herein referred to as SYNERGY). This has been shown to be an effective technique in other previous studies of deep convection (Romero et al., 1998; Homar et al., 2003; van den Heever et al., 2006). It is important to stress that SYNERGY is not merely the sum of RADIATION and DUST MICRO, but rather it is an additional contribution that is purely due to the nonlinear interactions between the two forcing mechanisms.

Let us consider a simple, hypothetical example that demonstrates a single synergistic contribution from a framework similar to the research herein. It is well known that dust acts as IN and that anvil clouds radiatively cool near cloud top due to longwave emission by condensate, mainly in the form of ice. From this, it could be expected that the sole inclusion of radiative transfer in a nocturnal squall line simulation (i.e. RADIATION) would act to cool the anvil, thereby increasing supersaturation and facilitating ice crystal growth. Similarly, it could be expected that the impacts of the sole inclusion of dust (i.e. DUST MICRO) on the anvil would act to increase ice crystal number concentrations and subsequently alter the ice crystal size distributions and microphysical processes within the anvil. Now, the synergistic contribution from radiative transfer

ACPD
12, 29607–29655, 2012

and dust (i.e. SYNERGY) within the anvil is more complex, as nonlinear interactions often occur. For example, because radiative cooling enhances supersaturation in the anvil, the additional cooling may help to nucleate more dust particles relative to the situation in which only the inclusion of dust is considered. The additional ice crystals produced through this synergistic response may then act to further enhance cloud top cooling over and above from that produced in RADIATION due to increases in ice crystal surface area and number concentration. This hypothetical example represents one possible nonlinear interaction that may result from the sensitivity experiments herein.

In order to fully quantify the three previously discussed contributions to the squall line (RADIATION, DUST MICRO, and SYNERGY), four sensitivity experiments are conducted in which the inclusion of radiation and microphysically active dust are systematically toggled. The description and name of each simulation is shown in Table 1, where the following information further describes the experiments:

- when dust is microphysically active, the full dust scheme is used and includes dust nucleating as liquid drops and ice crystals, dry deposition, and precipitation scavenging;
- when dust is not microphysically active, then dry deposition and precipitation scavenging are the only dust removal mechanisms;
- when radiation is turned off, the tendencies to the temperature field from radiative processes are not included; furthermore, radiation is not allowed to interact with the microphysics.

In order to most effectively isolate the AIE using factor separation on the four simulations, dynamic surface interaction is excluded for all simulations and is replaced by fixed values of surface temperature (300 K) and soil moisture (35 % volumetric content). Additionally, as the focus of the study is on aerosol indirect effects and not aerosol direct effects, *dust and sulfates are not radiatively active for all simulations*. A constant roughness length of 0.05 is used to simulate the effects of surface friction over grass

ACPD
12, 29607–29655, 2012

and brush, which is a common land surface for MCSs in semi-arid regions (Masson et al., 2003). Coriolis forcing is also excluded for all experiments to keep the squall line flow predominantly perpendicular to the meridionally oriented cold pool for more straightforward analysis.

The calculations used to isolate the factors described above are shown in Table 2, along with the naming convention that is used throughout the remaining sections. The term "the factor(s)" refers to the contributions to the squall line from the calculations of RADIATION, DUST MICRO, and SYNERGY (Table 2), and *not* the simulations of dOffrOff, dOnrOff, dOffrOn, and dOnrOn (Table 1). These calculations are applied to the group of simulations in a variety of ways (e.g. domain averaged fields, cloudy region averages, etc.) and will be described with respect to each analysis type.

3 Results

This section presents results from factor separation analyses of four simulations of an idealized nocturnal squall line. In order to provide a controlled set up of the experiment, a single squall line simulation was used as the benchmark squall line for the sensitivity experiments. This benchmark simulation is run for two hours and includes the full dust scheme and the effects of radiation. After two hours, the squall line has matured and the model is restarted using those data as the initial conditions for each of the four sensitivity experiments: dOffrOff, dOnrOff, dOffrOn, and dOnrOn (Table 1). For those analyses in this section that utilize time averaging, the first hour of each sensitivity experiment has been excluded in order to provide sufficient time for the squall line physics to evolve from the benchmark simulation. Furthermore, some of the analyses provided in this section are susceptible to local "shifts" of microphysical processes. Because of these shifts, zonally averaged values are also provided and discussed in order to obtain bulk assessments of the presented analyses. The results in this section are compartmentalized into two subsections that first describe the changes in the general characteristics and dynamics of the squall line due to the factors, and then describe the microphysics and thermodynamics responsible for those changes.

3.1 General characteristics and dynamics

The four squall line evolutions are consistent and characterized as a classic trailing stratiform squall line (Parker and Johnson, 2000). Figure 3 shows 1 km a.g.l. simulated radar reflectivity (Matrosov, 1999) and surface winds for the squall lines after one, three, and five hours into each simulation. It can be seen that all four squall lines have a leading line of high reflectivity that is trailed by a ~100 km wide region of lower reflectivity, consistent with the categorization of MCS's (Houze, 1993; Parker and Johnson, 2000). It can also be seen that the squall lines that include microphysically active dust (dOnrOff and dOnrOn) begin with stronger reflectivity values leading the convective line, but at the end of time integration, the two squall lines appear to be breaking up and weakening (compare Fig. 3c, f with Fig. 3i, l).

To begin the assessment of squall line intensity, Fig. 4 shows the contributions to precipitation from the factors as meridionally averaged Hovmöller diagrams, along with the full precipitation field of the CONTROL simulation (dOffrOff). The CONTROL simulation exhibits the classic characteristics of accumulated precipitation for a trailing stratiform squall line, where (1) a narrow region of enhanced precipitation occurs at the leading edge due to warm-rain formation, and (2) a precipitation minimum occurs behind the convective line (often referred to as the transition zone) that is followed by another local maximum in precipitation from ice processes (Fig. 4a). Including the effects of radiation (RADIATION; Fig. 4b) acts to increase precipitation for the entire squall line on average by up to 25 %, consistent with other studies (Tao et al., 1991, 1993; Dharssi et al., 1997). The inclusion of microphysically active dust (DUST MICRO) contributes to the precipitation field in three ways (Fig. 4c): (1) it initially enhances convective precipitation (up through the first 2.5 h); (2) it systematically decreases the stratiform precipitation; and (3) it reduces the domain mean precipitation during the second half of the experiment by up to 30 %. Furthermore, the synergistic contribution to precipitation from

ACPD
12, 29607–29655, 2012

microphysically active dust and radiation (SYNERGY; Fig. 4d) is not overall very large, and is characterized by a brief increase in precipitation between hours two and three followed by a decrease towards the end of time integration by up to 15 %.

The cold pool has been shown to play an integral role in the organization and structure of squall lines (Thorpe et al., 1982; Rotunno et al., 1988, 1990; Weisman et al., 1988; Weisman, 1992, 1993; Weisman and Rotunno, 2004, 2005; Bryan et al., 2006). To assess each factor's contribution to the cold pool speed of the squall line, a traditional measure of cold pool speed is used (e.g. Rotunno et al., 1988; Weisman and Rotunno, 2004; Bryan et al., 2006) that is based on density current theory and is given by (Benjamin, 1968)

$$C_B^2 = 2\int_0^H (-B)\mathrm{d}z \tag{1}$$

where C_B represents the cold pool propagation speed based, H represents the depth of the cold pool, and B represents buoyancy, which is calculated following Tompkins (2001). The cold pool boundary is defined by the $-0.05\,\mathrm{m^2\,s^{-2}}$ buoyancy surface. The speed of the cold pool of CONTROL (Fig. 5a) ranges from ~ 15–23 $\mathrm{m\,s^{-1}}$, and agrees well with other studies using the same thermodynamic profile as the squall line simulations here (e.g. Weisman and Rotunno, 2004; Bryan et al., 2006).

The factor separation analysis for cold pool speed shows perhaps unsurprisingly, a similar trend to precipitation for the contributions of RADIATION, DUST MICRO and SYNERGY (Fig. 5). On average, RADIATION generally does not contribute to a substantial change in cold pool speed until the final hour of the experiment, whereby an increase of up to 8 % occurs (Fig. 5b). DUST MICRO acts to initially increase the cold pool speed for the first hour; and is then followed by a decrease in cold pool speed throughout the remainder of time integration (Fig. 5c). SYNERGY's contribution to cold pool speed is overall not large and contains a maximum change in C_B of ~ 5 % (Fig. 5d).

ACPD
12, 29607–29655, 2012

This small change in cold pool speed is largely due to the small changes in condensate due to SYNERGY, which will be discussed in greater detail in the next subsection.

It has been shown that cold pool intensity and precipitation of squall lines are both dependent on various microphysical processes (Morrison et al., 2009, 2012; Bryan and Morrison 2012; Adams-Selin et al., 2012; van Weverberg et al., 2012). As such, in order to obtain a bulk perspective of the microphysics governing the squall line, Fig. 6 shows factor separation analyses of domain-averaged condensate paths and latent heating. The contributions to liquid water path (LWP) show consistent trends in time relative to CONTROL, whereby RADIATION increases LWP by up to 13 %, DUST MICRO removes up to ∼28 % of LWP, and SYNERGY has an oscillatory and overall neutral contribution to LWP. With respect to ice processes, RADIATION shows a systematic increase in ice water path (IWP) in time; and at the end of experiment RADIATION contributes up to a 22 % increase in IWP. An increase in squall line ice due to the inclusion of longwave radiation has also been seen by Tao et al. (1991, 1993), and will be further investigated later in this section. Both DUST MICRO and SYNERGY show a largely oscillatory response in contribution to IWP, except during the last hour where DUST MICRO dramatically reduces the IWP of the squall line, which is primarily due to the demise of the dOnrOff squall line from the significant weakening of the surface cold pool (Fig. 3i). The total water path (TWP) contributions from the factors indicate that RADIATION increases TWP (up to 14 %), DUST MICRO reduces TWP (up to 28 %), and SYNERGY again has an oscillatory contribution with small changes in time.

The changes in TWP will contribute to differences in latent heating (LH) that can alter the dynamics and intensity of the squall line. As such, a troposphere depth-normalized, vertically integrated LH rate is shown in Fig. 6d to gain a bulk perspective of LH. Similar to TWP, RADIATION invigorates the squall line latent heating and contributes to an enhancement of up to 26 %. DUST MICRO has a neutral contribution to latent heating through the first 2.5 h, as opposed to an expected negative contribution based on the decrease in TWP during this time. This discrepancy is explained by DUST MICRO's

ACPD
12, 29607–29655, 2012

contribution to precipitation, where an enhancement in the convective precipitation during the first 2.5 h effectively removed the water from the squall line that already contributed to the total latent heating. The SYNERGY contributions to latent heating are relatively insignificant and have an oscillatory nature.

To better understand how the factors are contributing to the structure and organization of the squall line, Fig. 7 shows vertical profiles of various temporally and domain averaged fields from cloud base (~ 1 km a.g.l.) up to just below the tropopause (~ 10 km a.g.l.), which are expressed as percent contributions to the squall line. The zonal wind field (U; Fig. 7a) of CONTROL has the classic structure of a well-organized squall line that is contributing to convective momentum transport (CMT; Lane and Moncrieff, 2010). This can be seen by a local maximum in $U \sim 3$ km a.g.l. due to the rear-to-front flow of the rear inflow jet (RIJ), and a local minimum in U within the anvil region ~ 7 km a.g.l. due to the front-to-rear (FTR) flow of the squall line within the updraft. As such, a positive contribution to the RIJ or a negative contribution to the FTR flow enhances the mesoscale organization of the squall line. From Fig. 7a, it can be seen that RADIATION most positively contributes to the CMT of the squall line, which is consistent with other previous studies (Chen and Cotton, 1988; Dudhia, 1989; Chin, 1994; Dharssi et al., 1997). DUST MICRO significantly weakens the kinematic organizational structure of the squall line, which corroborates the demise of the dOnrOff squall line due to a weaker cold pool. While SYNERGY has thus far indicated no significant contribution to the squall line, it has a slightly positive contribution to the CMT of the squall line.

The mean vertical velocity (W; Fig. 7b) of CONTROL is positive everywhere and peaks in the middle troposphere. The contribution to W by RADIATION is generally positive throughout the depth of the troposphere, except near the top of the anvil where longwave cooling produces sinking motion. DUST MICRO negatively contributes to W up through 5 km a.g.l., but positively contributes to W within the 5–9 km a.g.l. layer, indicating that ice processes may be playing a large role. SYNERGY slightly increases

ACPD
12, 29607–29655, 2012

the low-level $W \sim 3$ km a.g.l. and slightly decreases W around 6 km a.g.l., which may highlight a change to convective organization of the squall line.

By sampling the squall line for grid cells that have strong updrafts and strong downdrafts, a more in-depth assessment of squall line invigoration and convective organization can be made. Figure 7c shows the profile of total mass flux (MF), sampled where updrafts are greater than 2 m s^{-1} (i.e. convective mass flux, CMF). It is evident that RADIATION acts to enhance the CMF by up to 18 %. DUST MICRO decreases the CMF substantially throughout the troposphere, while SYNERGY generally has a neutral contribution to CMF except near the freezing level where it increases CMF by up to 8 % at ∼ 4 km a.g.l. Conversely, by sampling the squall line where vertical velocity is less than −1 m s^{-1}, Fig. 7d shows the mean downdraft mass flux (DMF) profile that helps to both transport momentum towards the surface from aloft and enhance the cold pool (Smull and Houze, 1987; Weisman, 1992). Where the CONTROL mesoscale downdraft is maximized (2–4 km a.g.l.), RADIATION positively contributes to DMF, DUST MICRO negatively contributes to DMF by up to 30 %, and SYNERGY positively contributes to DMF. The contributions by the factors to both CMF and DMF match well with the contributions by the factors to the zonal wind, further confirming that DUST MICRO reduces CMT while SYNERGY enhances CMT. The reasons for these contributions are due to changes in microphysical processes and will be discussed in the next subsection.

From this subsection, the two factors involved with the mineral dust AIE on a nocturnal squall line, DUST MICRO and SYNERGY, act to weaken and slightly strengthen the squall line, respectively. Because the contributions due to SYNERGY are relatively small, the combined contributions of DUST MICRO and SYNERGY lead to an overall weakening of the squall line in the presence of mineral dust. Conversely, the contribution of RADIATION is shown to invigorate the simulated squall line and matches well with past studies. The following subsection will explain in detail the microphysical processes responsible for the behavior of the factors (RADIATION, DUST MICRO, and SYNERGY) just discussed.

ACPD
12, 29607–29655, 2012

Squall line dust indirect effects

R. B. Seigel et al.

3.2 Microphysical response

Before analyzing the microphysical processes responsible for the behaviors of each factor just described, it is necessary to illustrate and describe how mineral dust is processed microphysically within the squall line. Figure 8 shows a meridionally and temporally averaged view of the dOnrOn squall line experiment. The microphysical processing of mineral dust acting as CCN by the squall line begins by nucleating cloud and drizzle drops in the inflow region of the squall line (Fig. 8a). The dust within cloud and drizzle (Fig. 8b) can then be tracked through the warm rain process as collision-coalescence generates raindrops (Fig. 8c). This process ultimately removes much of the dust through precipitation and may help to explain why DUST MICRO weakens the squall line due to a loss of potential IN. However, some dust remains within cloud, drizzle, and rain that can be followed to hail through riming processes near the freezing level within the updraft (Fig. 8d; Seigel and van den Heever, 2012b).

A second pathway of dust processing by the squall line occurs when dust acts as IN, and first occurs as pristine ice crystals nucleate near cloud top (Fig. 8e). Through vapor deposition, pristine ice grows into snowflake size crystals (Fig. 8f). As the snow containing dust sedimentates lower and resides longer in the anvil, ice crystal aggregation occurs because of increased probability of collection (Fig. 8g). The larger aggregates are transported rearward, while sedimentating towards the freezing level where increased riming by supercooled droplets can occur. This changes the dust-laden aggregates into graupel particles containing dust once sufficient riming has occurred (Fig. 8h). In the wake of the squall line surrounding the freezing level, a portion of the ice particles, snow, aggregates, graupel, and hail can sublimate, thereby releasing the dust particles back into the atmosphere as regenerated aerosol (Fig. 8i).

A factor separation analysis has been performed on each hydrometeor species' domain averaged path (i.e. a density-weighted, vertically-integrated mass) in order to gain insight into the microphysical processes responsible for the changes in dynamics discussed in the previous subsection. The contributions to each hydrometeor's mass by the factors are expressed as a percent change relative to CONTROL (Fig. 9). RADIATION increases the mass of all the hydrometeor types and adds 6 % to the total condensate of the squall line. DUST MICRO negatively contributes to each hydrometeor species' mass with a total condensate contribution of −16 %, which is predominantly due to the liquid species. SYNERGY's contribution is predominantly positive, however the total condensate contribution is small (less than 1 %) and is mainly due to changes in ice mass.

As a first step in the understanding of why these changes in condensate are occurring due to radiative and microphysical impacts by the factors, Fig. 10 shows a temporally- and meridionally- (following the gust front) averaged vertical cross section of the total condensate mixing ratio (TMIX) distribution within the squall line. Relative to CONTROL (Fig. 10a), it can be seen that the factors alter the TMIX distribution of the squall line in multiple ways. RADIATION increases TMIX throughout the depth of the troposphere (Fig. 10b). This is maximized near cloud top (30 % increase) due to cloud top radiational cooling (Fig. 11) that acts to destabilize the anvil region (Churchill and Houze, 1991), thereby promoting increased ice supersaturation that helps to grow condensate by vapor deposition. Additionally, a local maximum in TMIX enhancement occurs ~3 km a.g.l. that appears to lead to heavier precipitation shaft. This matches well with the overall increase in precipitation (Fig. 4b) and cold pool intensity (Fig. 5b), indicating that enhanced precipitation production leads to increased evaporational cooling that drives a stronger cold pool and squall line.

Consistent with the individual contributions to hydrometeor mass, DUST MICRO decreases the zonally averaged total condensate throughout the depth of the troposphere. Locally, DUST MICRO increases TMIX near the gust front, decreases the trailing stratiform precipitation, and greatly reduces TMIX just below the freezing level in the wake of the cold pool-forced updraft (Fig. 10c). It is interesting that while an increase in condensate occurs near the gust front, the cold pool intensity weakens due to DUST MICRO. This further highlights the importance of the ice phase in maintaining cold pool intensity through melting and sub-cloud evaporation, as the precipitation

ACPD
12, 29607–29655, 2012
Squall line dust indirect effects
R. B. Seigel et al.

originating from ice processes is reduced (∼ −20–30 km from GF in Fig. 10c). The physics governing these responses in the squall line TMIX will be discussed in more detail later in this section.

For SYNERGY, while large positive and negative contributions occur locally, its average contribution to TMIX is relatively minor (Fig. 10d). However, there is a general increase in TMIX (1) just above the freezing level, which is due to an increase in hail mass (Fig. 9), and (2) near cloud top which is due to an increase in mass of the ice hydrometeor species that predominantly grow by vapor deposition, pristine ice, snow, and aggregates (Fig. 9).

The changes in TMIX from DUST MICRO are largely due to the increase in warm rain production (Fig. 12). As dust is ingested by the squall line near cloud base (Fig. 8a), which has been shown to be the dominant source region of aerosol ingestion (Tulet et al., 2010; Seigel and van den Heever, 2012a), nucleation of both cloud and drizzle drops occurs that broadens the total distribution of liquid drops. This helps to speed up the collision-coalescence process that generates rain-sized drops. This can be seen by the up to 50 % increase in the cloud-to-rain process (CL2RT) just above the gust front (Fig. 12c). The rapid production of rain removes liquid from the squall line that could otherwise help to increase latent heating higher up in the updraft (notice 50 % reduction in mean TMIX near the freezing level in Fig. 10c). SYNERGY also enhances CL2RT near the gust front and is due to the strengthening of the cold pool-forced updraft (∼ 1–1.5 km a.g.l. in Fig. 7c) that increases supersaturation, leading to increased nucleation of both large and small dust particles (discussed later) that promotes greater collision-coalescence (Fig. 12d). While CL2RT also increases for RADIATION (Fig. 12b), this is because the squall line (dOffrOn) overall is stronger (relative to dOffrOff) and has a faster updraft below the freezing level (Fig. 7c), which increases CL2RT due to both enhanced turbulence and increased condensation (discussed later).

The increase in CL2RT for DUST MICRO removes liquid from the squall line that had the potential to be lofted higher into the storm to aid ice processes. As such, a reduction in riming of hail (the species that incurs the most riming; RIMHT) is evident

ACPD
12, 29607–29655, 2012

for DUST MICRO (Fig. 13c) in spatial collocation with those regions where significant riming occurs in CONTROL (Fig. 13a). Due to stronger 3–5 km a.g.l. mid-level updrafts from SYNERGY (Fig. 7c), an increase in RIMHT occurs just above the freezing level (Fig. 13d). The change in RIMHT for SYNERGY near the freezing level also matches the local changes in TMIX (Fig. 10d), indicating that the riming process is an important contributor to the increase in ice mass (Fig. 9). For RADIATION, riming is perhaps the most important microphysical process driving a stronger squall line. RADIATION dramatically increases RIMHT (Fig. 13b) throughout the depth of the mixed-phase region. This increase in riming is due to both an increase in liquid water (Fig. 9, 10b) and the increase in updraft strength above the freezing level (Fig. 7c), which increases riming rates.

In order to better understand how these changes to the microphysics from the factors alter the vertical distribution of LH, which lead to changes in squall line dynamics (Fovell and Ogura, 1988; Tao et al., 1995; Bryan and Morrison, 2012; Seigel and van den Heever, 2012b), a factor separation analysis of the LH budget of the squall line is shown in Fig. 14. RADIATION's contribution to the LH budget of the squall line is clear and matches well with the previous microphysical discussion (Fig. 14b). Radiative cooling near cloud top (Fig. 11) drives destabilization and increased ice supersaturation that helps to both nucleate more ice (ICE NUC) and grow more ice by vapor deposition (DEP) within the anvil at ~9–11 km a.g.l. The increase in ice condensate subsequently leads to an increase in melting (MELT), which helps to drive the stronger downdraft (Fig. 7d). This leads to a stronger cold pool (Fig. 5b) and stronger low-level updrafts (Fig. 7c) that increase supersaturation, resulting in a subsequent increase of condensation by up to 41 %. The increase in liquid condensate (Fig. 9) forces an increase in the contribution of riming to LH by 13 %. All of these microphysical processes act to strengthen the squall line.

Below the freezing level, DUST MICRO highlights the energetic ease of droplet growth versus droplet nucleation. First described by Squires and Twomey (1960), an increase in CCN assuming constant LWC results in a decrease in droplet size but an

ACPD
12, 29607–29655, 2012

Squall line dust indirect effects

R. B. Seigel et al.

increase in droplet number, and is also seen here in dOnrOff and dOnrOn relative to dOffrOff and dOffrOn (comparison not shown). As the change in droplet number occurs due to the addition of nucleating aerosol (dust), this increases the droplet surface area. Because the energy barrier to diffuse vapor onto an already present droplet is less than that to nucleate a dry aerosol (Prupacher and Klett, 1997), the process of vapor diffusion (COND) takes precedence over droplet nucleation (C + D NUC) on average. This effect has been noted by other aerosol modeling studies of aerosol impacts on deep convection (Storer and van den Heever, 2012; Sheffield et al., 2012) and is also seen for DUST MICRO, whereby the increase in C + D NUC below the freezing level is less than that of COND (Fig. 14c). However, the summation of the contribution by these two sources of LH from DUST NUC, which is maximized below the freezing level, positively contributes to the squall line by ∼ 42 %. This agrees well with many AIE studies that show increases in CCN lead to increases in droplet growth due to condensation (Khain et al., 2008; Lee et al., 2008b; Storer and van den Heever 2012).

Because mineral dust acts as IN, a 37 % increase in ICE NUC is also evident near cloud top, however DUST MICRO's net contribution to vapor deposition (DEP) is a mere 2.83 %. The reason why this contribution is not larger is due to the increase in warm rain (Fig. 11) scouring available water vapor that could have been used to grow ice crystals. The increase in condensation that leads to the invigoration of warm rain precipitation (Fig. 12c) reduces riming by 28 %, which has shown to be important for squall line maintenance (Seigel and van den Heever, 2012b).

SYNERGY's LH contributions to the squall line helps to explain why it contributes positively to the mid-level organization of the squall line. As the stronger cold pool-forced updraft (∼ 1–1.5 km a.g.l. in Fig. 7c) increases supersaturation, it leads to an increase in nucleation near cloud base at ∼ 1.5 km a.g.l. (Fig. 14d) that slightly enhances the warm-rain process (Fig. 12d). The slight rain increase of up to 10 % in this region (Fig. 10d) leads to the removal of the largest drops that temporarily shuts down the warm-rain process higher up ∼ 3 km a.g.l. (Fig. 12d). Because the precipitating droplets are removed, the surface area to volume ratio increases and promotes

ACPD
12, 29607–29655, 2012

greater condensational growth (COND) within the updraft, especially within the 3–5 km a.g.l. layer. The localized positive contribution to LH near the freezing level helps to drive a stronger mid-level updraft (Fig. 7c) that positively contributes to CMT (Fig. 7a). The stronger mid-level updraft then leads to a stronger mid-level downdraft (Fig. 7d) that increases melting by up to 6 %, and further contributes positively to CMT. Seigel and van den Heever (2012b) also found that enhanced latent heating near the freezing level helps to invigorate mesoscale organization of squall lines.

4 Summary

The goal of this study is to understand how mineral dust impacts a nocturnal squall line by separating out individual factors that contribute to the aerosol indirect effect. Using the technique of factor separation (Stein and Alpert, 1993), the contributions of mineral dust acting to alter microphysics (DUST MICRO), radiation (RADIATION), and the synergy of dust altering microphysics and radiation (SYNERGY) have been assessed for the squall line. This has been accomplished by using RAMS to simulate an idealized squall line with observed aerosol data from the NAMMA field campaign. Four simulations of the squall line were performed that systematically altered (1) the inclusions of dust acting microphysically (as CCN, GCCN, and IN) and (2) the inclusion of radiation (Table 1). Factor separation was then used to isolate three factors (RADIATION, DUST MICRO, and SYNERGY; Table 2) from the four simulations that contribute to the squall line.

The experiments showed that the overall role of mineral dust in the squall line simulated here is to weaken the squall line through changes to precipitation processes. From DUST MICRO, it has been shown that as the mineral dust is ingested into the squall line it acts as both CCN (mainly small dust mode) and GCCN (mainly large dust mode), which accelerates the collision-coalescence process of warm rain production. This has been seen by other studies of warm clouds in polluted environment (Feingold et al., 1999; Cheng et al., 2009). The increase in warm rain near the gust front due to DUST MICRO results in a reduction in liquid water aloft and reduces the contribution to latent heating by riming by up to 30 %, which weakens the main updraft of the squall line. The contribution from DUST MICRO to the mid-level portion of the squall line is also to decrease ice mass and weaken the mesoscale downdraft. The combination of weaker updrafts and downdrafts from DUST MICRO reduces the convective momentum transport and the overall squall line organization. In association with these processes, the cold pool is weaker, precipitation is reduced, and the total convective mass flux along with net latent heating is suppressed.

In contrast to the microphysical impacts of mineral dust, the role of RADIATION is to invigorate the squall line. This first begins by aiding ice nucleation and ice growth by vapor deposition due to the enhanced cloud top cooling by outgoing longwave radiation. The increase in ice mass due to RADIATION helps strengthen the mesoscale downdraft of the squall line, which enhances the convective momentum transport, surface cold pool, and precipitation. These all combine to then strengthen the low-level updrafts, which enhance supersaturation that aids condensation and additional latent heat release. This further strengthens the mesoscale organization of the squall line and promotes a positive feedback that is likely initiated from cloud top cooling.

By quantifying the individual contributions to the squall line due to DUST MICRO and RADIATION, it was then possible to assess the SYNERGY contribution to the squall line. SYNERGY represents the non-linear component of the AIE and is the result of the synergistic response to the squall line by having both radiation included and microphysically active dust present. While the overall contribution by SYNERGY to the squall line is small, it is positive for mesoscale organization. This stems from a change to the mid-level microphysical processes of the squall line due to SYNERGY. By having a slightly stronger low-level updraft, additional dust is nucleated by SYNERGY that enhances the warm-rain process just enough to remove the largest rain droplets while still maintaining sufficient droplet surface area to promote extra condensation. The additional latent heating by condensation near the freezing level facilitates a stronger mid-level updraft. This increases melting and results in a stronger mid-level downdraft. The

ACPD
12, 29607–29655, 2012

stronger mid-level dynamics promotes better mid-level organization, but is not strong enough to significantly impact precipitation and cold pool intensity.

As the squall line simulated in this study is nocturnal, only the impacts of long-wave forcing are considered. During the day, the presence of shortwave radiation may change the impact of both the mineral dust AIE and radiation on the simulated squall line. Therefore, current research is underway to examine the sensitivity of squall lines to mineral dust AIE during the daytime.

Acknowledgements. This work was jointly funded by the National Aeronautics and Space Administration under grant NNX07AT11G and the National Science Foundation under grant ATM-0820556.

References

Adams-Selin, R., van den Heever, S. C., and Johnson, R.: Impact of Graupel Parameterization Schemes on Idealized Bow Echo Simulations, Mon. Weather Rev., doi:10.1175/MWR-D-12-00064.1, in press, 2012a.

Adams-Selin, R., van den Heever, S. C., and Johnson, R.: Quantitative evaluation of bow echo microphysical sensitivity, Weather Forecast., in review, 2012b.

Albrecht, B. A.: Aerosols, cloud microphysics, and fractional cloudiness, Science, 245, 1227–1230, 1989.

Alpert, P., Tsidulko, M., and Stein, U.: Can sensitivity studies yield absolute comparisons for the effect of several processes?, J. Atmos. Sci., 52, 597–601, 1995.

Alpert, P. and Sholokhman, T. (Eds.): Factor Separation in the Atmosphere, Cambridge University Press, 352 pp., 2011.

Anderson, C. J. and Arritt, R. W.: Mesoscale convective complexes and persistent elongated convective systems over the US during 1992 and 1993, Mon. Weather Rev., 126, 578–599, 1998.

Andreae, M. O., Rosenfeld, D., Artaxo, P., Costa, A. A., Frank, G. P., Longo, K. M., and Silva-Dias, M. A. F.: Smoking rain clouds over the amazon, Science, 303, 1337, doi:10.1126/science.1092779, 2004.

Bangert, M., Nenes, A., Vogel, B., Vogel, H., Barahona, D., Karydis, V. A., Kumar, P., Kottmeier, C., and Blahak, U.: Saharan dust event impacts on cloud formation and radiation over Western Europe, Atmos. Chem. Phys., 12, 4045–4063, doi:10.5194/acp-12-4045-2012, 2012.

Benjamin, T. B.: Gravity currents and related phenomena, J. Fluid Mech., 31, 209–248, 1968.

Berg, W., L'Ecuyer, T., and van den Heever, S. C.: Evidence for the impact of aerosols on the onset and microphysical properties of rainfall from a combination of satellite observations and cloud-resolving model simulations, J. Geophys. Res, 113, D14S23, doi:10.1029/2007JD009649, 2008.

Borys, R. D., Lowenthal, D. H., Wetzel, M. A., Herrera, F., Gonzalez, A., and Harris, J.: Chemical and microphysical properties of marine stratiform cloud in the North Atlantic, J. Geophys. Res., 103, 22073–22085, 1998.

Bryan, G. H., Knievel, J. C., and Parker, M. D.: A multimodel assessment of RKW theory's relevance to squall-line characteristics, Mon. Weather Rev., 134, 2772–2792, 2006.

Bryan, G. H., Rotunno, R., and Fritsch, J. M.: Roll circulations in the convective region of a simulated squall line, J. Atmos. Sci., 64, 1249–1266, 2007.

Bryan, G. H. and Morrison, H.: Sensitivity of a simulated squall line to horizontal resolution and parameterization of microphysics, Mon. Weather Rev., 140, 202–225, doi:10.1175/MWR-D-11-00046.1, 2012.

Carrio, G. G., van den Heever, S. C., and Cotton, W. R.: Impacts of nucleating aerosol on anvil-cirrus clouds: a modeling study, Atmos. Res., 84, 111–131, 2007.

Chen, S. and Cotton, W. R.: The sensitivity of a simulated extratropical mesoscale convective system to longwave radiation and ice-phase microphysics, J. Atmos. Sci., 45, 3897–3910, 1988.

Cheng, W. Y. Y., Carrio, G. G., Cotton, W. R., and Saleeby, S. M.: Influence of cloud condensation and giant cloud condensation nuclei on the development of precipitating trade wind cumuli in a large eddy simulation, J. Geophys. Res., 114, D08201, doi:10.1029/2008JD011011, 2009.

Chin, H.-N. S.: The impact of the ice phase and radiation on a midlatitude squall line system, J. Atmos. Sci., 51, 3320–3343, 1994.

Churchill, D. D. and Houze Jr., R. A.: Effects of radiation and turbulence on the diabatic heating and water budget of the stratiform region of a tropical cloud cluster, J. Atmos. Sci., 48, 903–922, 1991.

Cotton, W. R., Pielke Sr., R. A., Walko, R. L., Liston, G. E., Tremback, C. J., Jiang, H., McAnelly, R. L., Harrington, J. Y., Nicholls, M. E., Carrio, G. G., and McFadden, J. P.: RAMS 2001: Current status and future directions, Meteorol. Atmos. Phys., 82, 5–29, 2003.

de Boer, G., Hashino, T., and Tripoli, G. J.: Ice nucleation through immersion freezing in mixed-phase stratiform clouds: theory and numerical simulations, Atmos. Res., 96, 315–324, 2010.

DeMott, P. J., Sassen, K., Poellet, M. R., Baumgardner, D., Rogers, D. C., Brooks, S. D., Prenni, A. J., and Kreidenweis, S. M.: African dust aerosols as atmospheric ice nuclei, Geophys. Res. Lett., 30, 1732, doi:10.1029/2003GL017410, 2003.

DeMott, P. J., Prenni, A. J., Lui, X., Kreidenweis, S. M., Petters, M. D., Twohy, C. H., M. Richardson, S., Eidhammer, T., and Rogers, D. C.: Predicting global atmospheric ice nuclei distributions and their impacts on climate, P. Natl. Acad. Sci., 107, 11217–11222, doi:10.1073/pnas.0910818107, 2010.

Dharssi, I., Kershaw, R., and Tao, W. K.: Sensitivity of a simulated tropical squall line to long-wave radiation, Q. J. Roy. Meteor. Soc., 123, 187–206, 1997.

Dudhia, J.: Numerical study of convection observed during the Winter Monsoon Experiment using a mesoscale two-dimensional model, J. Atmos. Sci., 46, 586–601, 1989.

Feingold, G. and Heymsfield, A. J.: Parameterizations of condensational growth of droplets for use in general circulation models, J. Atmos. Sci., 49, 2325–2342, 1992.

Feingold, G., Tzivion, S., and Levin, Z.: Evolution of raindrop spectra. Part I: Solution to the stochastic collection/breakup equation using the method of moments. J. Atmos. Sci., 45, 3387–3399, 1988.

Feingold, G., Walko, R. L., Stevens, B., and Cotton, W. R.: Simulations of marine stratocumulus using a new microphysical parameterization scheme, Atmos. Res., 47–48, 505–528, 1998.

Feingold, G., Cotton, W. R., Kreidenweis, S. M., and Davis, J. T.: The impact of giant cloud condensation nuclei on drizzle formation in stratocumulus: implications for cloud radiative properties, J. Atmos. Sci., 56, 4100–4117, 1999.

Ferek, R. J., Garrett, T., Hobbs, P. V., Strader, S., Johnson, D., Taylor, J. P., Nielsen, K., Ackerman, A. S., Kogan, Y., Liu, Q., Albrecht, B. A., and Babb, D.: Drizzle suppression in ship tracks. J. Atmos. Sci., 57, 2707–2728, 2000.

Fierro, A. O., Leslie, L. M., Mansell, E. R., and Straka, J. M.: Numerical simulations of the microphysics and electrification of the weakly electrified 9 February 1993 TOGA COARE squall line: comparisons with observations. Mon. Weather Rev., 136, 364–379, 2008.

Flatau, P. J., Tripoli, G. J., Verlinde, J., and Cotton, W. R.: The CSU-RAMS Cloud Microphysical Module: General Theory and Code Documentation, Atmos. Sci. Pap., 451, Dept. of Atmos. Sci., Colorado State University, Fort Collins, CO 80523, 88 pp., 1989.

Forster, P., Ramaswamy, V., Artaxo, P., Berntsen, T., Betts, R., Fahey, D. W., Haywood, J., Lean, J., Lowe, D. C., Myhre, G., Nganga, J., Prinn, R., Raga, G., Schulz, M., and Van Dorland, R.: Changes in Atmospheric Constituents and in Radiative Forcing, in: Climate Change 2007: The Physical Science Basis. Contribution of Working Group I to the Fourth Assessment Report of the Intergovernmental Panel on Climate Change, edited by: Solomon, S., Qin, D., Manning, M., Chen, Z., Marquis, M., Averyt, K. B., Tignor, M., and Miller, H. L., Cambridge University Press, Cambridge, United Kingdom and New York, NY, USA, 2007.

Fovell, R. G. and Ogura, Y.: Numerical simulation of a midlatitude squall line in two dimensions, J. Atmos. Sci., 45, 3846–3879, 1988.

Frame, J. and Markowski, P.: The interaction of simulated squall lines with idealized mountain ridges, Mon. Weather Rev., 134, 1919–1941, 2006.

Harrington, J. Y.: The effects of radiative and microphysical processes on simulated warm and transition season Arctic stratus., Ph. D. dissertation, atmospheric science paper 637, Department of Atmospheric Science, Colorado State University, 289 pp., 1997.

Heymsfield, A. J. and McFarquhar, G. M.: Microphysics of INDOEX clean and polluted trade cumulus clouds, J. Geophys. Res., 106, 28653–28673, 2001.

Hill, G. E.: Factors controlling the size and spacing of cumulus clouds as revealed by numerical experiments, J. Atmos. Sci., 31, 646–673, 2001.

Homar, V., Romero, R., Stensrud, D. J., Ramis, C., and Alonso, S.: Numerical diagnosis of a small, quasi-tropical cyclone over the Western Mediterranean: dynamical vs. boundary factors, Q. J. Roy. Meteor. Soc., 129, 1469–1490, 2003.

Houze, Jr., R. A.: Cloud Dynamics, Academic Press, 573 pp., San Diego, CA, USA, 1993.

Igel, A. L., van den Heever, S. C., Naud, C. M., Saleeby, S. M., and Posselt, D. J.: Sensitivity of warm frontal processes to cloud-nucleating aerosol concentrations, J. Atmos. Sci., accepted, 2012.

IPCC: “Climate change 2001: the scientific basis”, Intergovernmental panel on climate change, available at: http://www.grida.no/climate/ipcc_tar/wg1/index.htm, 2001.

Jirak, I. L., Cotton, W. R., and McAnelly, R. L.: Satellite and radar survey of mesoscale convective system development, Mon. Weather Rev., 131, 2428–2449, 2003.

ACPD
12, 29607–29655, 2012

Kaufman, Y. J. and Nakajima, T.: Effect of Amazon smoke on cloud microphysics and albedo – analysis from satellite imagery, J. Appl. Meteor., 32, 729–744, 1993.
Khain, A. P., Ovtchinnikov, M., Pinsky, M., Pokrovsky, A., and Krugliak, H.: Notes on the state-of-the-art numerical modeling of cloud microphysics, Atmos. Res., 55, 159–224, 2000.
Khain, A. P., Rosenfeld, D., and Pokrovsky, A.: Aerosol impact on the dynamics and microphysics of deep convective clouds, Q. J. Roy. Meteor. Soc., 131, 2639–2663, 2005.
Khain, A. P., BenMoshe, N., and Pokrovsky, A.: Factors determining the impact of aerosols on surface precipitation from clouds: an attempt at classification, J. Atmos. Sci., 65, 1721–1748, 2008.
Klemp, J. B. and Wilhelmson, R. B.: The simulation of three-dimensional convective storm dynamics, J. Atmos. Sci., 35, 1070–1096, 1978.
Laing, A. G. and Fritsch, J. M.: The global population of mesoscale convective complexes, Q. J. Roy. Meteor. Soc., 123, 389–405, 1997.
Lane, P. T. and Moncrieff, M. W.: Characterization of momentum transport associated with organized moist convection and gravity waves, J. Atmos. Sci., 67, 3208–3225, 2010.
Lee, S. S., Donner, L., and Phillips, V.: Examination of aerosol effects on precipitation in deep convective clouds during the 1997 ARM summer experiment, Q. J. Roy. Meteor. Soc., 134, 1201–1220, 2008a.
Lee, S. S., Donner, L., Phillips, V., and Ming, Y.: The dependence of aerosol effects on clouds and precipitation on cloud-system organization, shear and stability, J. Geophys. Res., 113, D16202, doi:10.1029/2007JD009224, 2008b.
Lee, S. S., Donner, L. J., and Phillips, V. T. J.: Impacts of aerosol chemical composition on microphysics and precipitation in deep convection, Atmos. Res., 94, 220–237, doi:10.1016/j.atmosres.2009.05.015, 2009.
Li, G., Wang, Y., Lee, K.-H., Diao, Y., and Zhang, R.: The impacts of aerosols on development and precipitation of a mesoscale squall line, J. Geophys. Res., 114, D17205, doi:10.1029/2008JD011581, 2009.
Lilly, D. K.: On the numerical simulation of buoyant convection, Tellus XIV, 14, 148–172, 1962.
Lynn, B. H., Khain, A., Dudhia, J., Rosenfeld, D., Pokrovsky, A., and Seifert, A.: Spectral (bin) microphysics coupled with a mesoscale model (MM5): Part I, Model description and first results, Mon. Weather Rev., 133, 44–58, doi:10.1175/MWR-2840.1, 2005a.

Lynn, B. H., Khain, A., Dudhia, J., Rosenfeld, D., Pokrovsky, A., and Seifert, A.: Spectral (bin) microphysics coupled with a mesoscale model (MM5): Part I I. Simulation of a CaPE rain event with a squall line, Mon. Weather Rev., 133, 59–71, doi:10.1175/MWR-2841.1, 2005b.
Masson, V., Champeaux, J.-L., Chauvin, F., Meriguet, C., and Lacaze, R.: A global database of land surface parameters at 1-km resolution in meteorological and climate models, J. Climate, 16, 1261–1282, 2003.
Matrosov, S. Y.: Retrieval of vertical profiles of ice cloud microphysics from radar and IR measurements using tuned regressions between reflectivity and cloud parameters, J. Geophys. Res., 104, 16741–16753, 1999.
Matsui, T., Masunaga, H., Pielke, Sr., R. A., and Tao, W.-K.: Impact of aerosols and atmospheric thermodynamics on cloud properties within the climate system, Geophys. Res. Lett., 31, L06109, doi:10.1029/2003GL019287, 2004.
Meyers, M. P., Walko, R. L, Harrington, J. Y., and Cotton, W. R.: New RAMS cloud microphysics parameterization. Part II: The two-moment scheme, Atmos. Res, 45, 3–39, 1997.
Morrison, H.: On the robustness of aerosol effects on an idealized supercell storm simulated with a cloud system-resolving model, Atmos. Chem. Phys., 12, 7689–7705, doi:10.5194/acp-12-7689-2012, 2012.
Morrison, H. and Grabowski, W. W.: Comparison of bulk and bin warm-rain microphysics models using a kinematic framework, J. Atmos. Sci., 64, 2839–2861, 2007.
Morrison, H., Thompson, G., and Tatarskii, V.: Impact of cloud microphysics on the development of trailing stratiform precipitation in a simulated squall line: comparison of one- and two-moment schemes, Mon. Weather Rev., 137, 991–1007, 2009.
Morrison, H., Tessendorf, S. A., Ikeda, K., and Thompson, G.: Sensitivity of a Simulated Midlatitude Squall Line to Parameterization of Raindrop Breakup, Mon. Weather Rev., 140, 2437–2460. http://dx.doi.org/10.1175/MWR-D-11-00283.1doi:10.1175/MWR-D-11-00283.1, 2012.
Nesbitt, S. W., Cifelli, R., and Rutledge, S. A.: Storm morphology and rainfall characteristics of TRMM precipitation features, Mon. Weather Rev., 134, 2702–2721, doi:10.1175/MWR3200.1, 2006.
Parker, M. D. and Johnson, R. H.: Organizational modes of midlatitude mesoscale convective systems, Mon. Weather Rev., 128, 3413–3436, 2000.
Perry, K., Cahill, T., Eldred, R., Dutcher, D. D., and Gill, T. E.: Long-range transport of North African dust to the Eastern US, J. Geophys. Res., 102, 11225–11238, 1997.

ACPD
12, 29607–29655, 2012

Squall line dust indirect effects

R. B. Seigel et al.

Pielke, R. A., Cotton, W. R., Walko, R. L., Tremback, C. J., Lyons, W. A., Grasso, L. D., Nicholls, M. E., Moran, M. D., Wesley, D. A., Lee, T. J., and Copeland, J. H.: A comprehensive meteorological modeling system – RAMS, Meteor. Atmos. Phys., 49, 69–91, 1992.

Prospero, J. M.: Saharan dust transport over the North Atlantic Ocean and Mediterranean: an overview, in: The Impact of Desert Dust Across the Mediterranean, edited by: Guerzoni, S. and Chester, R., Kluwer Academic, Dordrecht, The Netherlands, 133–151, 1996.

Prospero, J. M.: Long-term measurements of the transport of African mineral dust to the Southeastern US: implications for regional air quality, J. Geophys. Res., 104, 15917–15927, 1999.

Pruppacher, H. R. and Klett, J. D.: Microphysics of Clouds and Precipitation, 2nd Edn., Kluwer Academic, Dordrecht, The Netherlands, 954 pp., 1997.

Romero, R., Ramis, C., Alonso, S., Doswell III, C. A., and Stensrud, D. J.: Mesoscale model simulations of three heavy precipitation events in the Western Mediterranean region, Mon. Weather Rev., 126, 1859–1881, 1998.

Rosenfeld, D.: Suppression of rain and snow by urban and industrial air pollution, Science, 287, 1793–1796, doi:10.1126/science.287.5459.1793, 2000.

Rosenfeld, D. and Feingold, G.: Explanation of the discrepancies among satellite observations of the aerosol indirect effects, Geophys. Res. Lett., 30, 1776, doi:10.1029/2003GL017684, 2003.

Rosenfeld, D., Lohmann, U., Raga, G., O'Dowd, C., Kulmala, M., Fuzzi, S., Reissell, A., and Andreae, M.: Flood or drought: how do aerosols a_ect precipitation? Science, 321, 1309–1313, 2008.

Rotunno, R., Klemp, J. B., and Weisman, M. L.: A theory for strong, long-lived squall lines, J. Atmos. Sci., 45, 463–485, 1988.

Rotunno, R., Klemp, J. B., and Weisman, M. L.: Comments on "A numerical investigation of the organization and interaction of the convective and tratiform regions of tropical squall lines.", J. Atmos. Sci, 47, 1031–1033, 1990.

Saleeby, S. M. and Cotton, W. R.: A large-droplet mode and prognostic number concentration of cloud droplets in the Colorado State University Regional Atmospheric Modeling System (RAMS), Part I: Module descriptions and supercell test simulations, J. Appl. Meteor., 43, 182–195, 2004.

Saleeby, S. M. and van den Heever, S. C.: Developments in the CSU-RAMS Aerosol Model: Emissions, Nucleation, Regeneration, Deposition and Radiation, J. Appl. Meteorol. Clim., submitted, 2012.

ACPD

12, 29607–29655, 2012

Sassen, K., DeMott, P. J., Prospero, J. M., and Poellet, M. R.: Saharan dust storms and indirect aerosol effects on clouds: CRYSTAL-FACE results, Geophys. Res. Lett., 30, 1633, doi:10.1029/2003GL017371, 2003.
Seifert, A. and Beheng, K. D.: A two-moment cloud microphysics parameterization for mixed-phase clouds, Part 2: Maritime vs. continental deep convective storms, Meteorol. Atmos. Phys., 92, 67–82, 2006.
Seigel, R. B. and van den Heever, S. C.: Dust lofting and ingestion by supercell storms, J. Atmos. Sci., 69, 1453–1473, 2012a.
Seigel, R. B. and van den Heever, S. C.: Squall line intensification via hydrometeor recirculation, J. Atmos. Sci., accepted, 2012b.
Sheffield, A. M., van den Heever, S. C., and Saleeby, S. M.: Growth of cumulus congestus clouds when impacted by aerosols, J. Atmos. Sci., accepted, 2012.
Smagorinsky, J.: General circulation experiments with the primitive equations, I. The basic experiment, Mon. Weather Rev., 91, 99–164, 1963.
Smull, B. F. and Houze Jr., R. A.: Rear inflow in squall lines with trailing-stratiform precipitation, Mon. Weather Rev., 115, 2869–2889, 1987.
Solomos, S., Kallos, G., Kushta, J., Astitha, M., Tremback, C., Nenes, A., and Levin, Z.: An integrated modeling study on the effects of mineral dust and sea salt particles on clouds and precipitation, Atmos. Chem. Phys., 11, 873–892, doi:10.5194/acp-11-873-2011, 2011.
Squires, P. and Twomey, S.: The relation between cloud drop spectra and the spectrum of cloud nuclei, in: Physics of Precipitation, Geophys. Monogr. Ser., vol. 5, edited by: Weickmann, H., AGU, Washington, D. C., 211–219, 1960.
Stein, U. and Alpert, P.: Factor separation in numerical simulations, J. Atmos. Sci., 50, 2107–2115, 1993.
Storer, R. L. and van den Heever, S. C.: Microphysical processes evident in aerosol forcing of tropical deep convection, J. Atmos. Sci., in press, 2012.
Storer, R. L., van den Heever, S. C., and Stephens, G. L.: Modeling aerosol impacts on convective storms in different environments, J. Atmos. Sci., 67, 3904–3915, 2010.
Tao, W., Simpson, J., and Soong, S.: Numerical simulation of a subtropical squall line over the Taiwan Strait, Mon. Weather Rev., 119, 2699–2723, 1991.
Tao, W., Simpson, J., Sui, C., Ferrier, B., Lang, S., Scala, J., Chou, M., and Pickering, K.: Heating, moisture and water budgets of tropical and mid-latitude squall lines: comparison and sensitivity to long-wave radiation, J. Atmos. Sci., 50, 673–890, 1993.

ACPD
12, 29607–29655, 2012

Tao, W., Scala, J. R., Ferrier, B., and Simpson, J.: The effect of melting processes on the development of a tropical and a midlatitude squall line, J. Atmos. Sci., 52, 1934–1948, 1995.
Tao, W., Chen, J.-P., Li, Z., Wang, C., and Zhang, C.: Impacts of aerosols on convective clouds and precipitation, Rev. Geophys., 50, RG2001, doi:10.1029/2011RG000369, 2012.
Tegen, I. and Fung, I.: Modeling of mineral dust in the atmosphere: sources, transport and optical thickness, J. Geoph. Res., 99, 22897–22914, 1994.
Thorpe, A. J., Miller, M. J., and Moncrieff, M. W.: Two-dimensional convection in non-constant shear: a model of midlatitude squall lines, Q. J. Roy. Meteor. Soc., 108, 739–762, 1982.
Tompkins, A. M.: Organization of tropical convection in low vertical wind shears: the role of cold pools, J. Atmos. Sci., 58, 1650–1672, 2001.
Trier, S. B., Skamarock, W. C., and LeMone, M. A.: Structure and evolution of the 22 February 1993 TOGA COARE squall line: organization mechanisms inferred from numerical simulations, J. Atmos. Sci., 54, 386–407, 1997.
Tulet, P., Crahan-Kaku, K., Leriche, M., Aouizerats, B., and Crumeyrolle, S.: Mixing of dust aerosols into a mesoscale convective system: generation, filtering and possible feedbacks on ice anvils, Atmos. Res., 96, 302–314, 2010.
Twohy, C. H., Kreidenweis, S. M., Eidhammer, T., Browell, E. V., Heymsfield, A. J., Bansemer, A. R., Anderson, B. E., Chen, G., Ismail, S., DeMott, P. J., and van den Heever, S C.: Saharan dust particles nucleate droplets in Eastern Atlantic clouds, Geophys. Res. Lett., 36, L01807, doi:10.1029/2008GL035846, 2009.
Twomey, S.: The influence of pollution on the shortwave albedo of clouds, J. Atmos. Sci., 34, 1149–1152, 1977.
van den Heever, S. C. and Cotton, W. R.: The impact of hail size on simulated supercell storms, J. Atmos. Sci., 61, 1596–1609, 2004.
van den Heever, S. C. and Cotton, W. R.: Urban aerosol impacts n downwind convective storms, J. Appl. Meteorol. Clim., 46, 828–850, doi:10.1175/JAM2492.1, 2007.
van den Heever, S. C., Carrió, G. G., Cotton, W. R., DeMott, P. J., and Prenni, A. J.: Impacts of nucleating aerosol on Florida storms, Part I: Mesoscale simulations, J. Atmos. Sci., 63, 1752–1775, 2006.
van den Heever, S. C., Stephens, G. L., and Wood, N. B.: Aerosol indirect effects on tropical convection characteristics under conditions of radiative-convective equilibrium, J. Atmos. Sci., 68, 699–718, doi:10.1175/2010JAS3603.1, 2011.

Van Weverberg, K., Vogelmann, A., Morrison, H., and Milbrandt, J.: Sensitivity of idealized squall line simulations to the level of complexity used in two-moment bulk microphysics schemes, Mon. Weather Rev., 140, 1883–1907, 2012.
Verlinde, J., Flatau, P. J., and Cotton, W. R.: Analytical solutions to the collection growth equation: comparison with approximate methods and application to cloud microphysics parameterization schemes, J. Atmos. Sci., 47, 2871–2880, 1990.
Walko, R. L., Tremback, C. J., Pielke, R. A., and Cotton, W. R.: An interactive nesting algorithm for stretched grids and variable nesting ratios, J. Appl. Meteorol., 34, 994–999, 1995.
Wang, C.: A model study of the response of tropical deep convection to the increase of CCN concentration: 1. Dynamics and microphysics, J. Geophys. Res., 110, D21211, doi:10.1029/2004JD005720, 2005.
Weisman, M. L.: The role of convectively generated rear-inflow jets in the evolution of long-lived mesoconvective systems, J. Atmos. Sci., 49, 1826–1847, 1992.
Weisman, M. L.: The genesis of severe, long-lived bow echoes, J. Atmos. Sci., 50, 645–670, 1993.
Weisman, M. L. and Klemp, J. B.: The dependence of numerically simulated convective storms on vertical wind shear and buoyancy, Mon. Weather Rev., 110, 504–520, 1982.
Weisman, M. L., Klemp, J. B., and Rotunno, R.: Structure and evolution of numerically simulated squall lines, J. Atmos. Sci., 45, 1990–2013, 1988.
Weisman, M. L. and Rotunno, R.: "A theory for strong long-lived squall lines" revisited, J. Atmos. Sci., 61, 361–382, 2004.
Weisman, M. L. and Rotunno, R.: Reply, J. Atmos. Sci., 62, 2997–3002, doi:10.1175/JAS3515.1, 2005.

ACPD
12, 29607–29655, 2012

Table 1. Description and naming convention of the four experiments.

Name	Description
dOffrOff	Dust being microphysically active is OFF Radiation is OFF
dOffrOn	Dust being microphysically active is OFF Radiation is ON
dOnrOff	Dust being microphysically active is ON Radiation is OFF
dOnrOn	Dust being microphysically active is ON Radiation is ON

ACPD
12, 29607–29655, 2012

Table 2. The components and naming convection of the factor separation analysis.

Factor	Name	Description	Calculation
f_0	CONTROL	Part of the predicted field independent from dust altering the microphysics and radiation	f_0 = dOffrOff
f_1	RADIATION	Part of the predicted field from the sole contribution of radiation	f_1 = dOffrOn – dOffrOff
f_2	DUST MICRO	Part of the predicted field from the sole contribution of dust altering the microphysics	f_2 = dOnrOff – dOffrOff
f_{12}	SYNERGY	Part of the predicted field from the synergistic effects of dust altering the microphysics *and* radiation	f_{12} = dOnrOn – (dOnrOff + dOffrOn) + dOffrOff

ACPD
12, 29607–29655, 2012

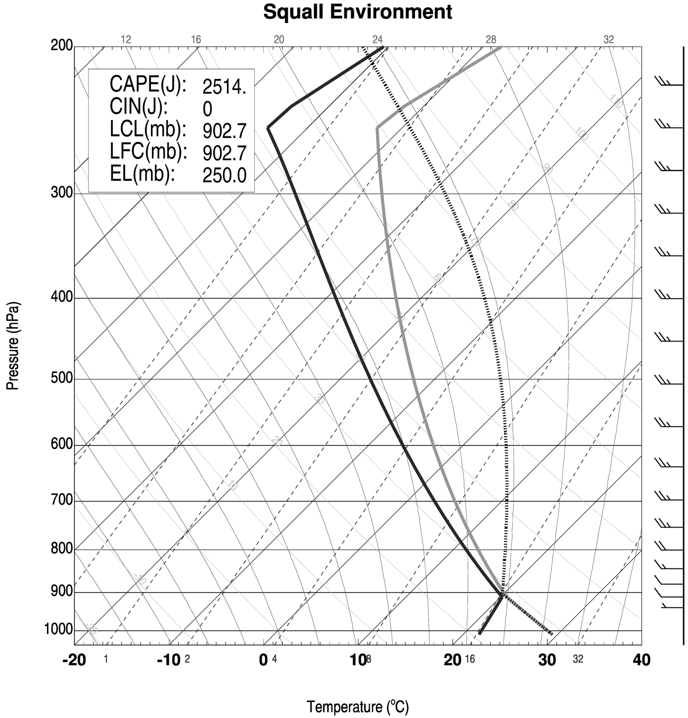

Fig. 1. Horizontally homogeneous environmental conditions initialized for the squall line. The thick grey line is the temperature profile and the thick black is the moisture profile. The thick dashed line is the adiabatic parcel curve. Following Weismann and Klemp (1982).

ACPD
12, 29607–29655, 2012

Squall line dust indirect effects

R. B. Seigel et al.

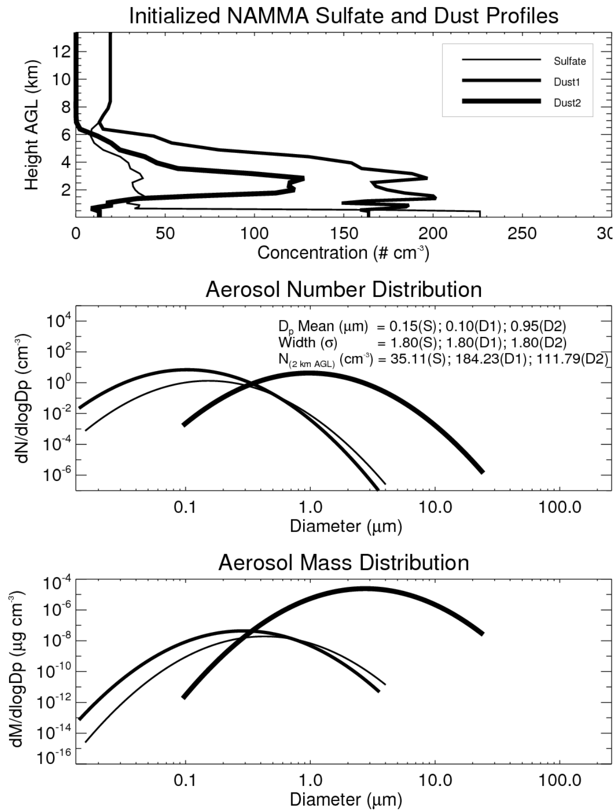

Fig. 2. Aerosol data from NASA African Monsoon Multidisciplinary Analyses (NAMMA) in 2006. The three aerosol species represented in the study are sulfate (thin), small dust (medium thickness), and large dust (thick). Top: the initialized horizontally-homogeneous profiles (cm^{-3}); middle: aerosol number distribution at 2 km a.g.l.; and bottom: aerosol mass distribution at 2 km a.g.l. Also shown on **(b)** are the geometric mean particle diameter, distribution width parameter, and the total number concentration for sulfate (S), Dust1 (D1), and Dust2 (D2).

ACPD
12, 29607–29655, 2012

Squall line dust indirect effects

R. B. Seigel et al.

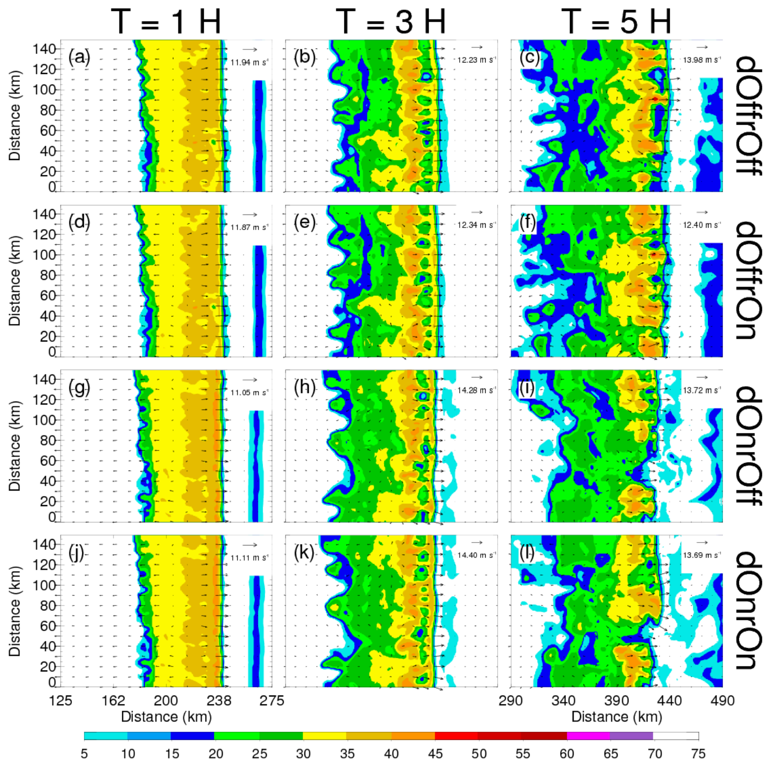

Fig. 3. Simulated base radar reflectivity (dBZ; Matrosov 1999) of dOffrOff **(a–c)**, dOffrOn **(d–f)**, dOnrOff **(g–i)**, and dOnrOn **(j–l)** at 1 km a.g.l. for: **(a, d, g, j)** $T = 1$ h; **(b, e, h, k)** $T = 3$ h; and **(c, f, i, l)** $T = 5$ h into the sensitivity simulations. The surface winds are shown (vectors) along with the maximum surface wind reference vector in the upper-right corner for each image.

ACPD
12, 29607–29655, 2012

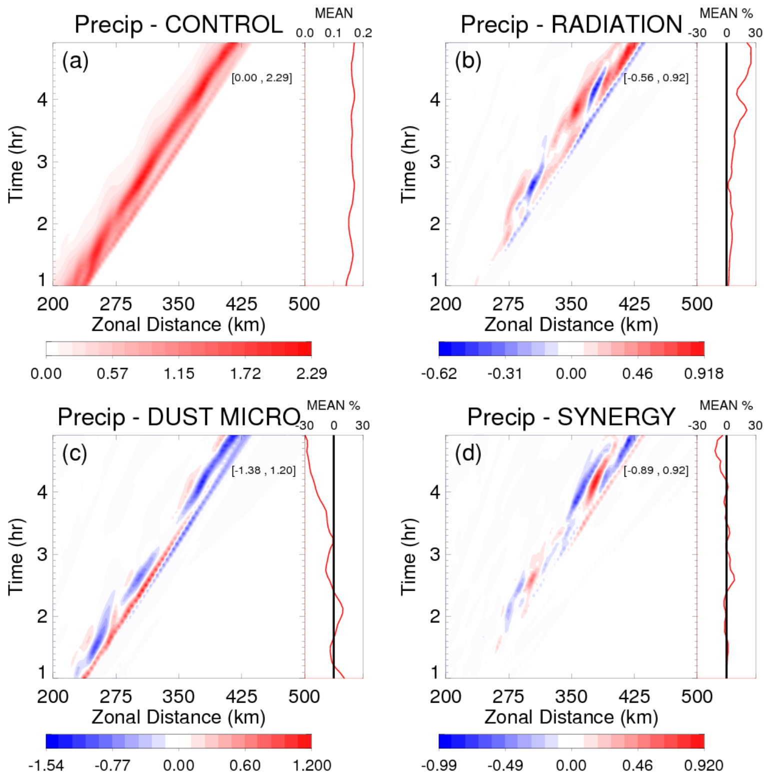

Fig. 4. Meridionally averaged accumulated precipitation (mm 5 min^{-1}) for the four factors of **(a)** CONTROL, **(b)** RADIATION, **(c)** DUST MICRO, and **(d)** SYNERGY. See Tables 1 and 2 for factor descriptions. The accumulated precipitation is expressed as a both a Hovmöller diagram (shading) and a zonally averaged time series that is expressed as a percent contribution relative to CONTROL (line plot).

ACPD
12, 29607–29655, 2012

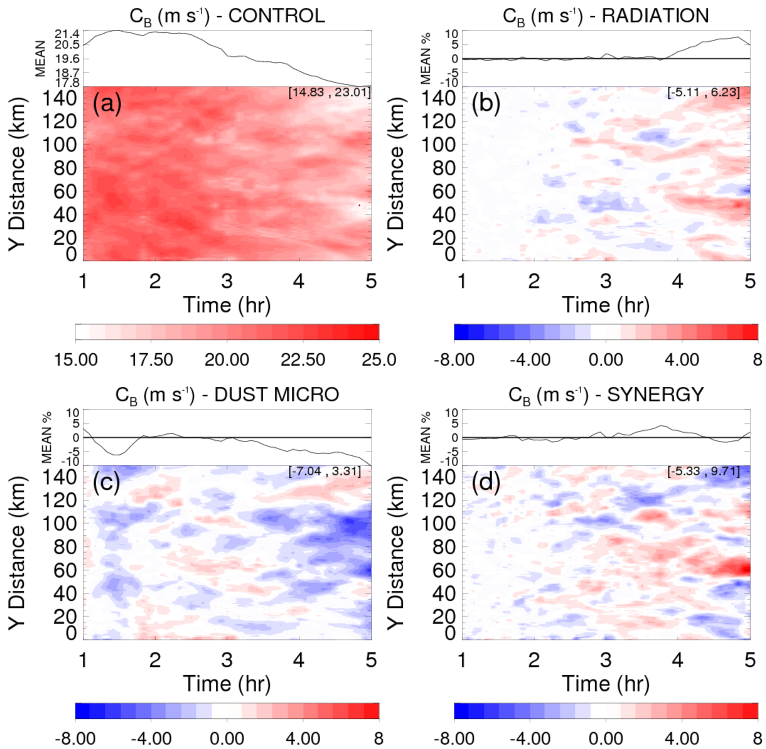

Fig. 5. Theoretical cold pool speed, which is defined in (1), shown for the four factors of **(a)** CONTROL, **(b)** RADIATION, **(c)** DUST MICRO, and **(d)** SYNERGY. The cold pool speed is expressed as a both a rotated Hovmöller diagram (shading) and a meridionally averaged time series that is expressed as a percent contribution relative to CONTROL (line plot).

ACPD

12, 29607–29655, 2012

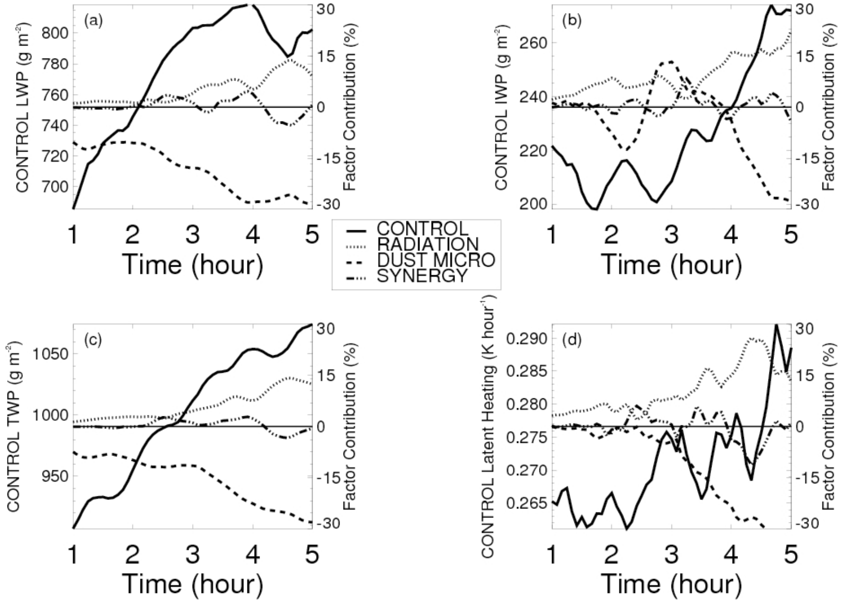

Fig. 6. Domain averaged time series of **(a)** liquid water path ($g\,m^{-2}$), **(b)** ice water path ($g\,m^{-2}$), **(c)** total water path ($g\,m^{-2}$), and **(d)** troposphere depth normalized, vertically integrated latent heating rate ($K\,h^{-1}$). The solid lines correspond to CONTROL with the full field values on the left axes. The dotted (RADIATION), dashed (DUST MICRO), and dot-dash (SYNERGY) lines correspond to the factors and are expressed as a percent contribution to CONTROL – shown on the right axes.

ACPD
12, 29607–29655, 2012

Title Page
Abstract Introduction
Conclusions References
Tables Figures
Back Close
Full Screen / Esc
Printer-friendly Version
Interactive Discussion

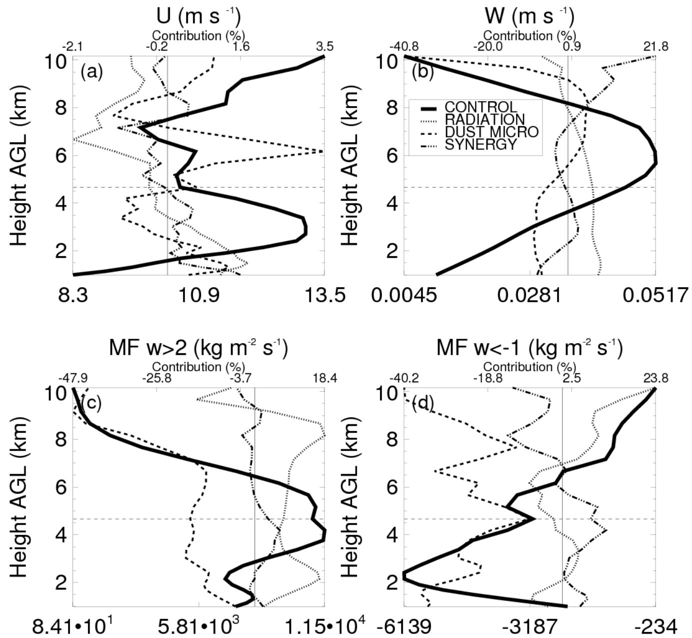

Fig. 7. Domain averaged vertical profiles of **(a)** zonal wind ($\mathrm{m\,s^{-2}}$), **(b)** vertical velocity ($\mathrm{m\,s^{-2}}$), **(c)** total convective mass flux sampled where $W > 2\,\mathrm{m\,s^{-2}}$ ($\mathrm{kg\,m^{-2}\,s^{-1}}$), and **(d)** total downdraft mass flux sampled where $W < -1\,\mathrm{m\,s^{-2}}$ ($\mathrm{kg\,m^{-2}\,s^{-1}}$). The solid lines correspond to CONTROL with the full field values on the bottom axes. The dotted (RADIATION), dashed (DUST MICRO), and dot-dash (SYNERGY) lines correspond to the factors and are expressed as a percent contribution to CONTROL on the top axes.

ACPD
12, 29607–29655, 2012

Title Page
Abstract | Introduction
Conclusions | References
Tables | Figures
◀I | ▶I
◀ | ▶
Back | Close
Full Screen / Esc
Printer-friendly Version
Interactive Discussion

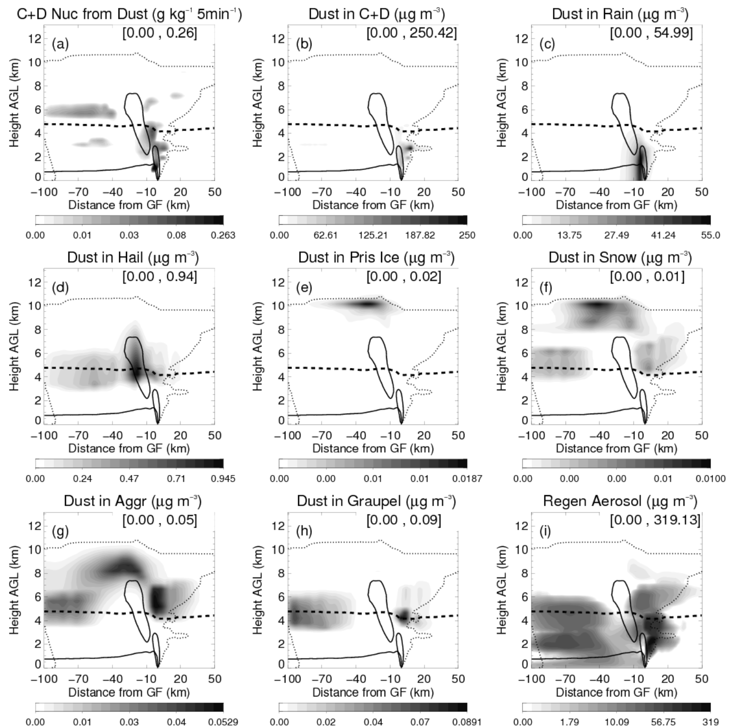

Fig. 8. The dOnrOn squall line, which has been averaged both meridionally along the gust front and temporally from sensitivity simulation hours 1–5. Each vertical cross section is expressed as a horizontal distance from the gust front (x-axis) and a vertical distance a.g.l. (y-axis). Shown on each cross section is the squall line cloud boundary (dotted line; 0.05 $\mathrm{g\,kg^{-1}}$ total condensate), the freezing line (dashed black line), the cold pool boundary (thin black line below 2 km a.g.l.; $-0.05\,\mathrm{m^2\,s^{-2}}$ following Tompkins, 2001), the 1 $\mathrm{m\,s^{-1}}$ updraft region (thick black lines stemming from the gust front), and (min, max) values for the shaded quantities of: **(a)** cloud and drizzle (C + D) nucleation rate by dust; **(b)** dust within C + D; **(c)** dust within rain; **(d)** dust within hail; **(e)** dust within pristine ice; **(f)** dust within snow; **(g)** dust within aggregates; **(h)** dust within graupel; and **(i)** concentration of regeneration aerosol. The units are shown on the figure for each quantitiy.

ACPD
12, 29607–29655, 2012

Squall line dust indirect effects

R. B. Seigel et al.

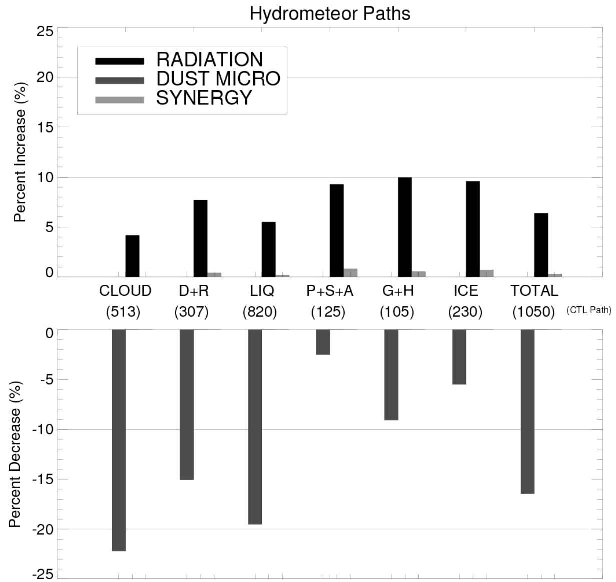

Fig. 9. Horizontally averaged, vertically integrated mixing ratios of various hydrometeors, referred to in the text as hydrometeor paths. The hydrometeor paths are expressed as a percent contribution to CONTROL by RADIATION (black bars), DUST MICRO (gray bars), and SYNERGY (light gray bars). D+R is drizzle and rain, P+S+A is pristine ice and snow and aggregates, and G+H is graupel and hail. The numbers below each hydrometeor group are the full field path value for CONTROL in g m^{-2}.

ACPD
12, 29607–29655, 2012

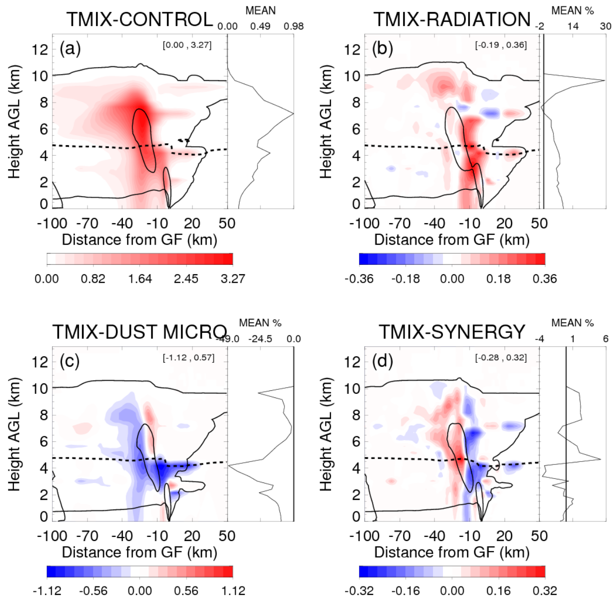

Fig. 10. Meridionally-averaged along the gust front and temporally-averaged total condensate mixing ratio (TMIX; $\mathrm{g\,kg^{-1}}$) for **(a)** CONTROL, **(b)** RADIATION, **(c)** DUST MICRO, and **(d)** SYNERGY from sensitivity simulation hours 1–5. Each vertical cross section is expressed as a horizontal distance from the gust front (x-axis) and a vertical distance a.g.l. (y-axis). Shown on each cross section is the squall line cloud boundary (thick black line; $0.05\,\mathrm{g\,kg^{-1}}$ total condensate), the freezing line (dashed black line), the cold pool boundary (thin black line below 2 km a.g.l.; $-0.05\,\mathrm{m^2\,s^{-2}}$) the $1\,\mathrm{m\,s^{-1}}$ updraft region (thick black "ovals" stemming from the gust front), and (min, max) values for TMIX. The cloud boundary, freezing level, cold pool, and updraft contours are of the simulations **(a)** dOffrOff, **(b)** dOffrOn, **(c)** dOnrOff, and **(d)** dOnrOn. Also shown is a zonally averaged vertical profile that is expressed as a percent contribution relative to CONTROL (line plot) for each factor.

ACPD
12, 29607–29655, 2012

Squall line dust indirect effects

R. B. Seigel et al.

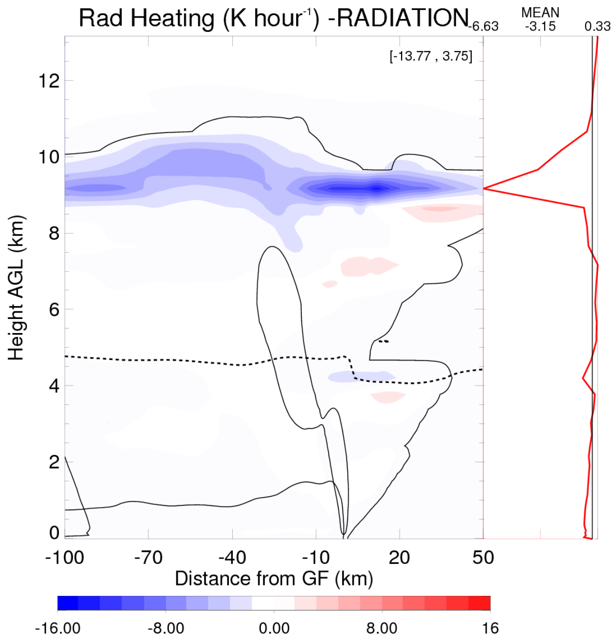

Fig. 11. Same as Fig. 10, except for radiative heating rate ($\mathrm{K\,h^{-1}}$) and only shown for RADIATION and dOffrOn.

ACPD
12, 29607–29655, 2012

Squall line dust indirect effects

R. B. Seigel et al.

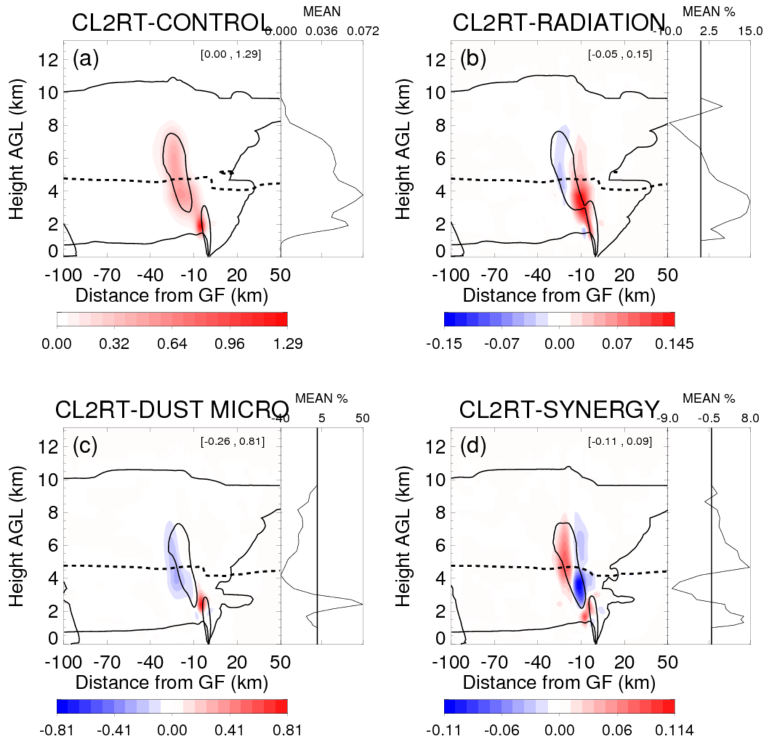

Fig. 12. Same as Fig. 10, except for the collision-coalescence rate ($g\,kg^{-1}\ 5\,min^{-1}$) between cloud and rain.

ACPD
12, 29607–29655, 2012

Squall line dust indirect effects

R. B. Seigel et al.

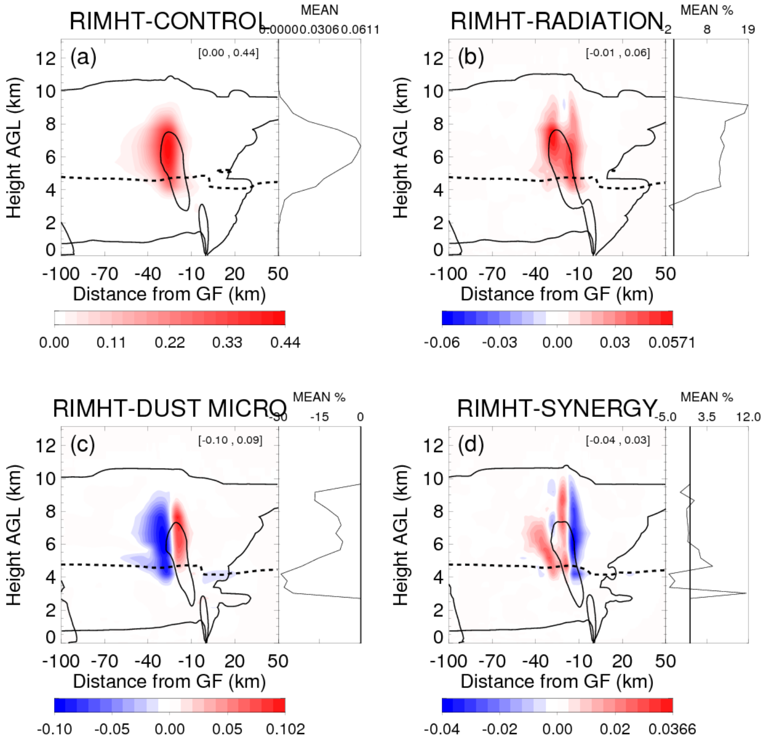

Fig. 13. Same as Fig. 10, except for the riming rate of cloud water onto hail ($\mathrm{g\,kg^{-1}\,5\,min^{-1}}$).

ACPD
12, 29607–29655, 2012

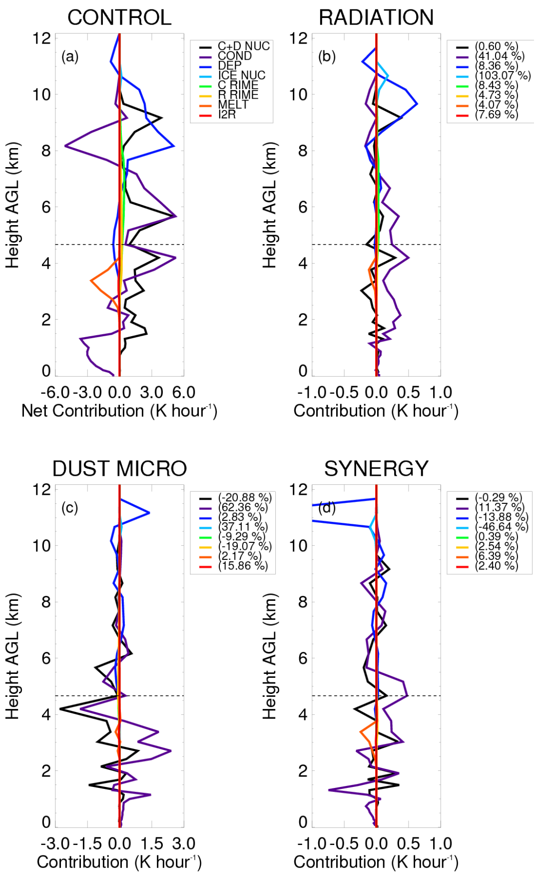

Fig. 14. Cloud averaged vertical profiles of all microphysical processes that contribute to latent heating ($\mathrm{K\,h^{-1}}$) for **(a)** CONTROL, **(b)** RADIATION, **(c)** DUST MICRO, and **(d)** SYNERGY. Cloud is defined by any grid cell that contains at least 0.01 $\mathrm{g\,kg^{-1}}$ of total condensate.

ACPD
12, 29607–29655, 2012

Squall line dust indirect effects

R. B. Seigel et al.